Investigation of Crack Propagation and Opening in Hydroxyapatite Using Digital Image Correlation

3 authors, including:

Mohamed mahdi Mahdi

University of Babylon

1 PUBLICATION   **0** CITATIONS

SEE PROFILE

Some of the authors of this publication are also working on these related projects:

Fracture Mechanics View project

Investigation of Crack Propagation and Opening in Hydroxyapatite Using Digital Image Correlation

Mohammed M. Hussien Albo-Jasim, Mohsin A. Aswad and Hayder K. Rashed
Department of Ceramic and Building Materials, College of Materials Engineering,
University of Babylon, Babylon, Iraq

Abstract: The effect of single edge notched beam on the fracture mechanics, for example, crack observation, initiation, opening and propagation of hydroxyapatite samples were investigated in this study. The strain evolution and cracking near the crack notch tip region on the strain map were in situ monitored using digital image correlation technique. The critical crack mouth and critical crack tip opening displacement were 40 and 17 μm, respectively at critical bending load about 10 N. Digital Image Correlation (DIC) technique was established as a good and very precise tool for fracture measurements such as crack opening and length.

Key words: Hydroxyapatite, crack propagation, crack opening, digital image, correlation, fracture mechanics

INTRODUCTION

Hydroxyapatite (HA, $Ca_{10}(PO_4)_6(OH)_2$ are primary candidates for hard tissue reconstruction as well as regeneration. Having similar chemical composition to the mineral component of natural bone HA is not only bioactive but also more biocompatible than any other ceramic (Pattanayak *et al.*, 2005; Eslami *et al.*, 2008; Tahriri *et al.*, 2008). Hydroxyapatite, a successful bioactive ceramic but exhibits poor mechanical properties especially fracture toughness limiting the usability of the material and preventing its use in major load bearing applications (Elghazel *et al.*, 2015). Crack Opening Displacement (COD) is a parameter describing the near-tip crack profile and predicting the fracture and is defined as the relative opening movement of the upper and lower crack flanks (Kanninen *et al.*, 1986). This parameter is one of the most used fracture criteria in which various studies have been proposed in literature (Newman *et al.*, 2003; Tagawa *et al.*, 2010; Li *et al.*, 2011). Fracture mechanics is the science of describing how a crack or a flaw occurs and propagates under applied loads in a structure. Cracks may occur in everywhere therefore application areas of fracture mechanics is extensive. The samples dimensions of brittle material to be tested is excessively minor to enable extensometers or electromechanical to be used for determining the displacement of the opening crack (Brynk *et al.*, 2012). Measuring the crack opening displacement is difficult and as values obtain smaller, distinct equipment is needed. For a ceramic, SEM and AFM have been utilized. These methods require precise sample preparation and distinctive care to determine accurate values of displacement (Lin *et al.*, 2016; Mekky and Nicholson, 2006). To overcome these obstacles a process for measuring the displacement of mini sample and accurate strain measurements may be achieved with non-contact optical method, namely Digital Image Correlation (DIC) which used to determine the displacement and strain of sample to detect crack propagation and measurement crack opening displacement (Brynk *et al.*, 2014). Many methods are currently used to measure the fracture toughness of ceramic materials. Methods based on accepted theories like Chevron Notch (CN), Surface Crack in Flexure (SCF) (Triwatana *et al.*, 2013), indentation techniques such as Indentation Fracture (IF) Indentation Strength (IS) (Anstis *et al.*, 1981). Single edge notched beam (SENB) method is a common method for measuring the fracture toughness of ceramics with standard 3-point bend loading of notched beams. The aim of this study is to visualization and monitoring the crack propagation in hydroxyapatite and measurement the crack mouth and crack tip opening displacement using digital image correlation technique.

MATERIALS AND METHODS

Preparation of the hydroxyapatite powder: Bovine femur bone was selected as the starting biosource material for production hydroxyapatite powder. The spongy bones were cut and the bone was defleshed. The bone marrow and all portions of meat and fat were isolated. Using a gas flame under direct ignition to the cleaned bone with temperature 700°C for 4 h, organic parts were charred.

Corresponding Author: Mohammed M. Hussien Albo-Jasim, Department of Ceramic and Building Materials, College of Materials Engineering, University of Babylon, Babylon, Iraq

Fig. 1: Polished sample

Fig. 2: Notched sample using

The product of this process producing some carbonizes due to burning of organic component. To remove the remaining char, the black powder (bone ash) was placed in an air furnace at temperature between 900°C for 3 h and finally, it was cooled inside the furnace. Following this process, the black ash turned into a white granular powder.

Preparation of the hydroxyapatite sample: Sample of hydroxyapatite powder was mixed with (2% wt.) Poly Vinyl Alcohol (PVA) as a binder's material. Uniaxial semi-dry pressing technique was employed for forming ceramic samples using a mold made of stainless steel with dimensions 60 mm in length and 6 in 5 mm in thickness. The appropriate pressure was 150 MPa, the green density was measured at this pressure close to theoretical density. Compacts samples were prepared by sintered at temperatures at 1250°C with heating rate (5°C/min) and soaking time 3 h and cooled inside the furnace. The samples were grinding at a speed 300 rev/min with SiC grinding papers 180, 320, 600, 800, 1200, 1000, 1500 and 2000 grit size. The time of grinding was 15 min for every grit size and using the water for coolant. After grinding, polishing process was accomplished using same machine but replace SiC paper with polishing cloth and using diamond paste as lubricated material. Figure 1 shows the polished sample.

Figure 2 showed the sample of HA in dimensions 3×4×50 mm and the sample prepared studying fracture using single edge notch beam. Notch was made using a 250 μm thick diamond-coated dental cutting disk the notch preform in 3 mm face. The fracture toughness of hydroxyapatite calculation according to ASTM C 1421.

Digital image correlation: DIC is a non-contacting optical and numerical method capable of accurately providing full-field, 2-Dimensional (2-D) and 3-Dimensional (3-D) displacements and strains. This deformation information is obtained by mathematically
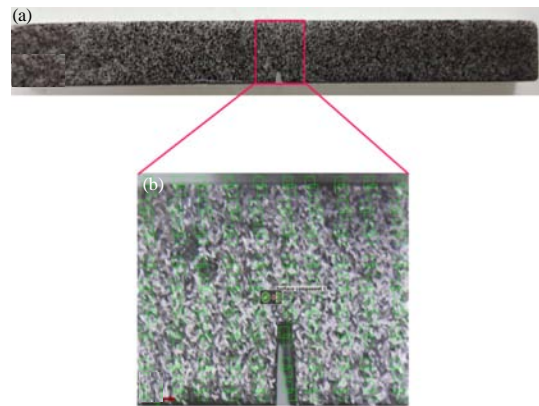

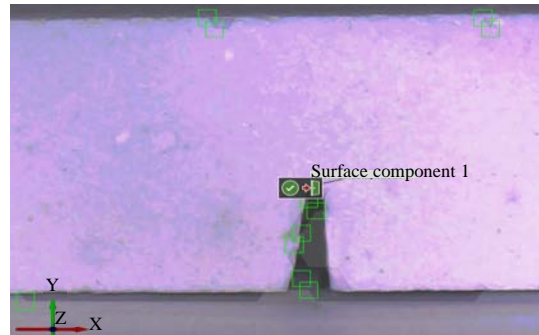Fig. 3: a) Speckles of black paint and b) Subset on the sample surface

Fig. 4: Specimen with no paint and there is no subset on its surface

tracking similar local features between images of an object's surface taken before and after deformation. Images are commonly captured in natural or white light environment making the method suitable for both laboratory and in-field applications. The method also has a wide range in applicable length scales that can range from the macro to nano-scale (Mathieu *et al.*, 2012; Roux *et al.*, 2009).

Experimental work: The artificial speckle pattern was created by sprayed randomly with a black paint on the specimen surface as shown in Fig. 3a. The speckle pattern is required to be non-repetitive, isotropic and contrast enough to permit the software to be able to identify and to match the image before and after deformation. A typical speckle pattern on the object is shown in Fig. 3b. The sprayed of sample is necessary to made subset, Fig. 4 show the sample without features (black and white paint), it can be notice from this figure no subset formation on the samples surface which is essential to work the program.
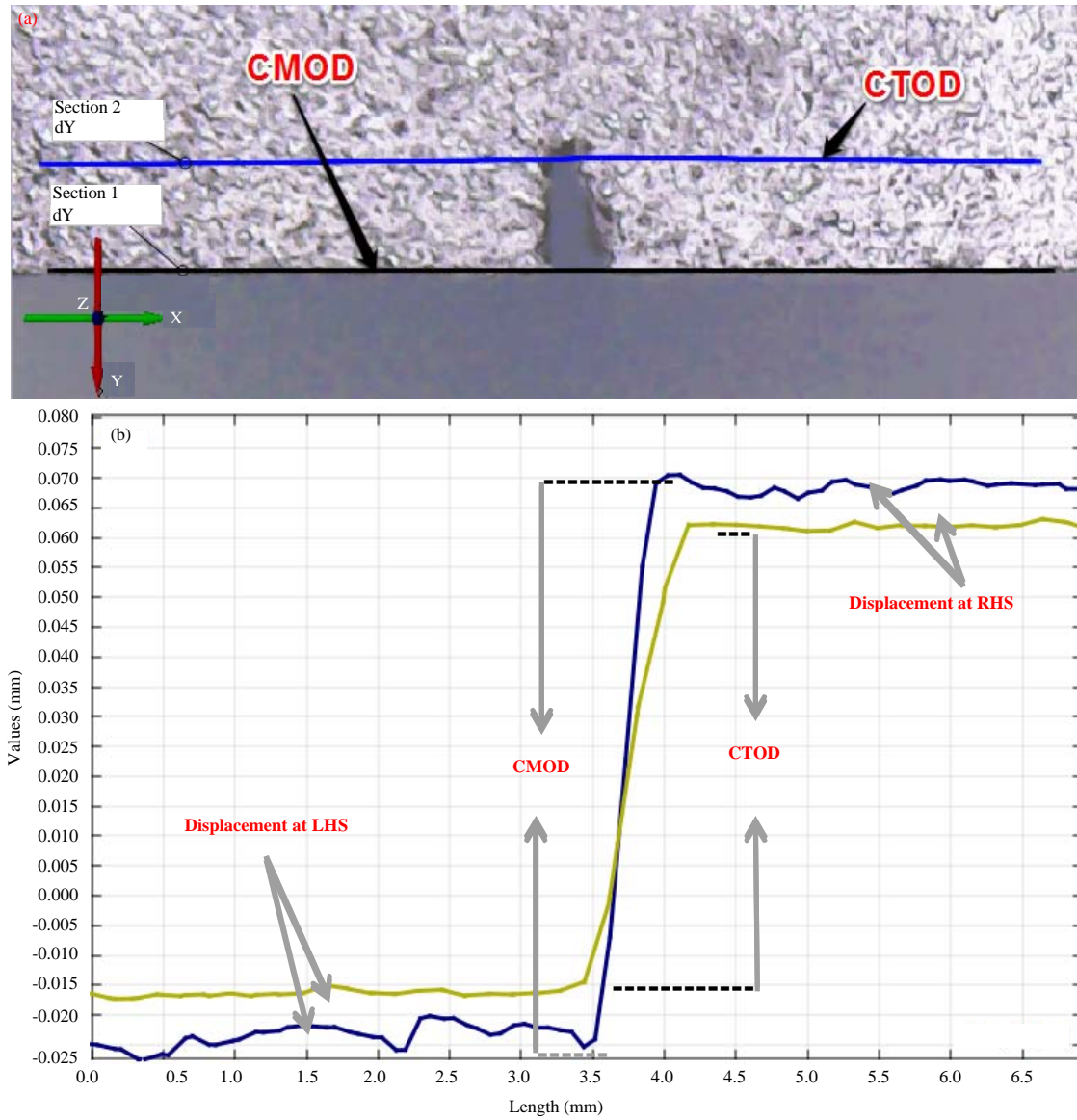
Fig. 5: a) Position of CMOD and CTOD and b) Measurement of CMOD and CTOD

The Software of DIC used for calculation named GOM (Gesellschaft fur Optische Mebtechnik) from a German company. This calculation technique starts with a reference image taken before loading which is compared with a series of pictures during the loading period. An assumption is proposed that the color value of the images remains the same before and after the deformation. First of all, select a Region of Interest (ROI) on the specimen surface as shown in Fig. 4-8; then, divide this region into numbers of subsets; search for the corresponding subsets after deformation based on the assumption and calculate their displacements; finally, a deformation or displacement distribution map is created. Specimens were
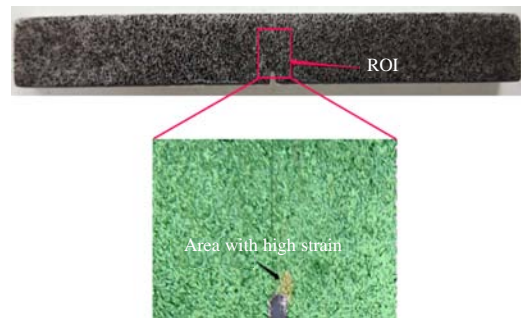

Fig. 6: Shows high strain area which refer to crack propagation
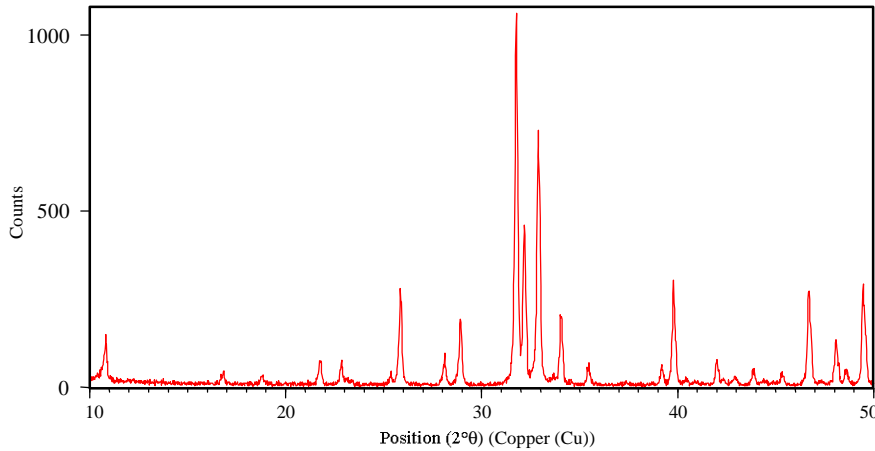
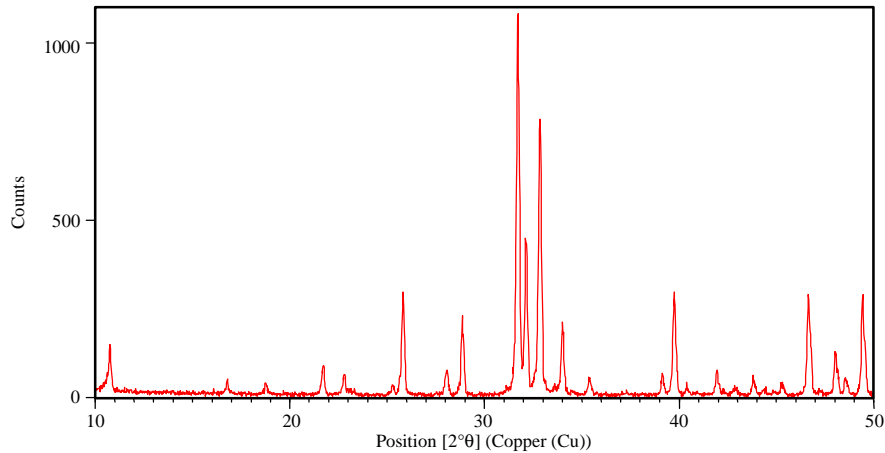Fig. 7: XRD of HA powder at 900°C

Fig. 8: XRD of HA sample at 1250°C

subjected to the load microcomputer controlled electronic universal testing machine (WDW-5E). This testing machine has a loading capacity of 5 KN and the loading rate is very low, resulting in a displacement not exceeding 0.005 mm/min. a digital microscope camera (Genesys logic) and this camera contain lamp which used to lighten the speckle pattern and adopted to acquire digital images during loading process. The camera position was adjusted to make its lens parallel to the specimen surface as much as possible and the focal length was also adjusted to make the image clear. The resolution of the camera was set to 640×480 pixels and the length-pixel ratio of the imaging system is 0.0008 mm/pixel. The camera was programmed to capture the images automatically at a frame rate 30 (30 pic/sec) and this frame rate is suitable to capture and to store a large number of images for further calculations.

The position of crack mouth and crack tip opening displacement can be notice in Fig. 5a. The Crack Opening Displacement (CMOD and CTOD) can be measure throw DIC using line profile horizontal displacement as shown in the Fig. 5a. The correlation algorithm determines the location of each sub-pixel in the imaging area. The horizontal (axial) displacement can be easily calculated from displacement contours. A sudden jump in the displacement values can be observed and it represents a discontinuity (crack) in the material. The crack opening calculation by subtracted LHS (Left Hand Side) displacement form displacement of RHS (Right Hand Side) as shown in the Fig. 5b.

In order to evaluate the crack propagation, the Region of Interesting (ROI) above the notch is taken into account. By taking the horizontal strain (ε_{xx}) to shows strain map which lead to identify crack

propagation and also can be determined crack position by taken the strain on line profile as shown in the Fig. 6.

RESULTS AND DISCUSSION

X-ray diffraction: X-ray diffraction technique was used to identify the phases that present in the materials, Fig. 7 shows the result of X-ray diffraction analysis of HA powder calcined at 900°C with a heating rate of 10°C /min and soaking time of 2 h. The result shows that all peaks corresponding with hydroxyapatite phase and matched with (JCPDS, Card No. 1-089-6440). The result of x-ray diffraction analysis of HA sample sintering at 1250°C with a heating rate of 7°C/min and soaking time of 3 h. For 1250°C the Fig. 8 shows no decomposition of hydroxyapatite and all peaks refers for hydroxyapatite and matched with (JCPDS, Card No. 01-089-6440).

Fourier transform infrared spectrometer: Figure 9 shows the FTIR test of HA and the broad band at 3437 and 1610 cm^{-1} were attributable to adsorb water while sharp beak at 3572 cm^{-1} was attributable to stretching vibration of lattice -OH ions and medium sharp peak at 632 cm^{-1} assign to the O-H deformation mode. The characteristic bands for PO_4^{-3} appear at 570, 601, 960, 1049 and 1089 cm^{-1}. The results show that the powders of hydroxyapatite free from carbonate groups. The result of FTIR of HA samples were correlated with reference (Berzina-Cimdina and Borodajenko, 2012).

Fracture toughness: The fracture toughness of hydroxyapatite measured with single edge notched beam method was 0.7 MPa. $\sqrt{m}$ and this value closed to the value of hydroxyapatite measured with another method such Vickers indentation method.

Digital image correlation
Crack observation: The results obtained from DIC to identified crack visualization with applied load. Figure 10 shows the change in strain mapping near the notch tip at different loads and times for hydroxyapatite sample. Figure 10a show the undeform sample (before applied loading), Fig. 10b don't shows any change in strain mapping near the notch tip, but the viewed area was deformed. Figure 10c shows change in strain mapping near the notch tip which indicated to stress concentration near the notch tip. At 210 sec and at load 10 N the crack has been initiated as shown in Fig. 10d. After time 210 sec the specimen losing the bearing capacity and load rabidly decrease when crack propagated as shown in Fig. 10e and f.

Crack opening displacement: The relationship between applied force and Crack Opening Displacement (CMOD and CTOD) as shown in Fig. 11 and represent the force versus CMOD curve can be divided to three parts .In the first part, the relationship is linear, the second part start as soon as the curve deviates from linearity. Crack opening starts to increase at faster rate indicating the development of damage in the material. In this part, the load continues to increase further until the peak load value is reached and the material cannot go beyond this maximum loading capacity. After the peak load stage, the last part start when crack mouth opening displacement continues to
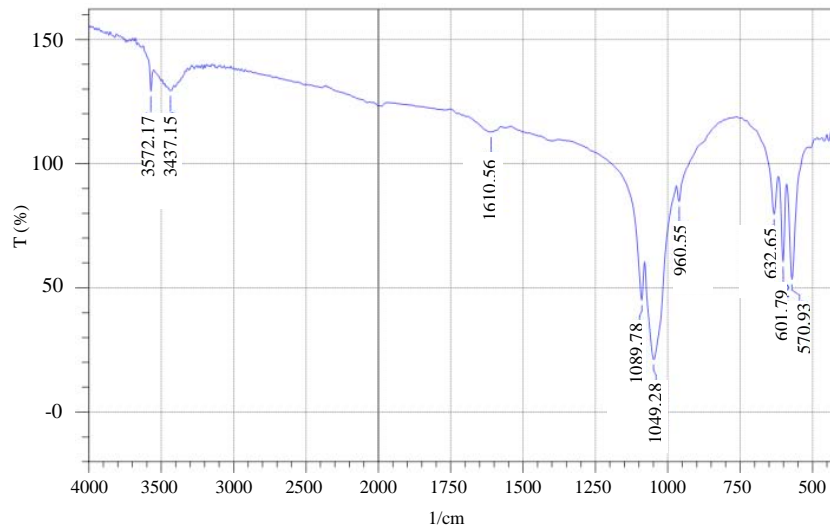

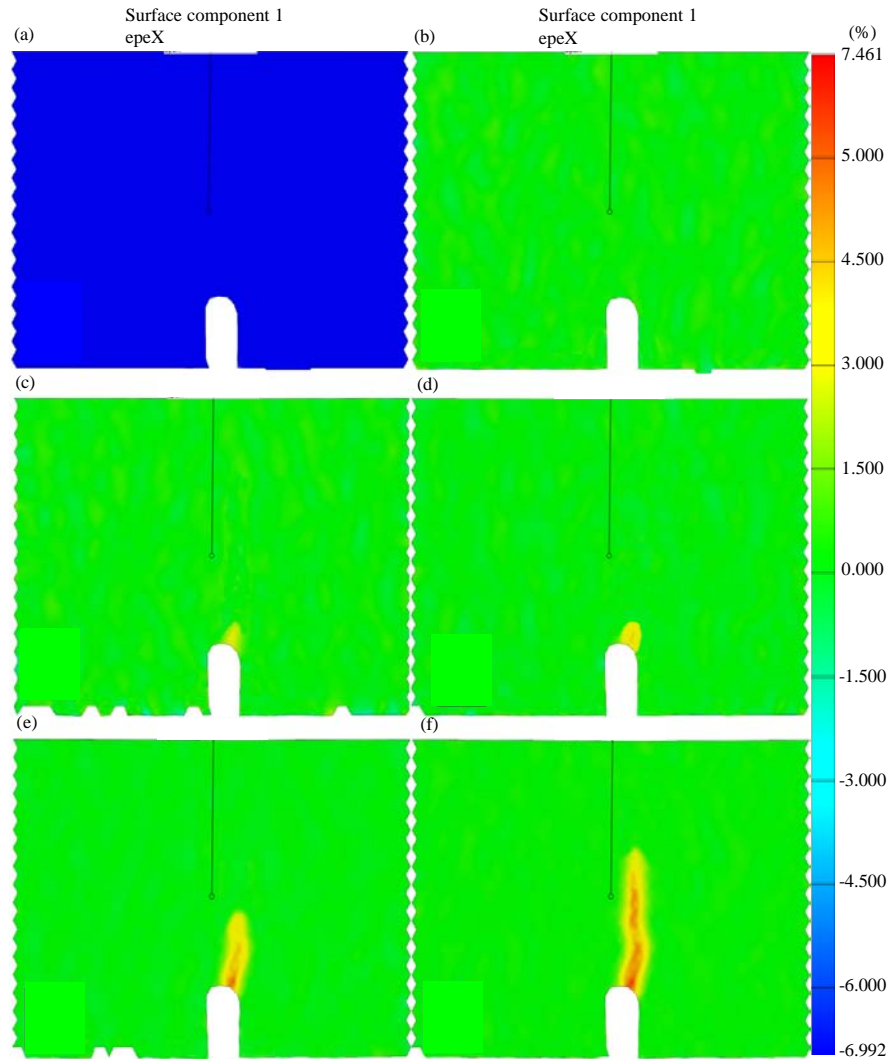Fig. 9: FTIR of HA powder calcination at 900°C

Fig. 10: Strain maps of HA with different load and time: a) P = 0 N, t = 0 sec; b) P = 4 N, t = 90 sec; c) P = 8 N, t = 195 sec; d) P = 10 N, t = 210 sec; e) P = 6.5 N, t = 560 sec and f) P = 3.6 N, t = 860 sec
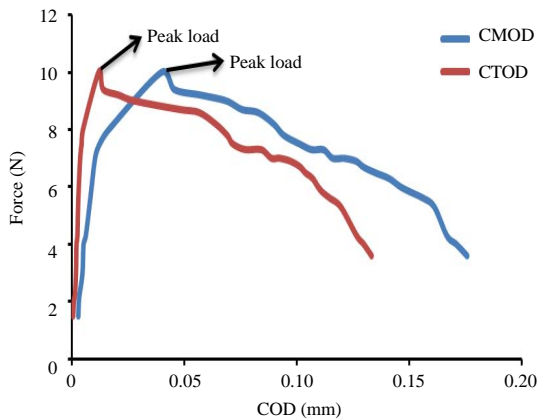

Fig. 11: Force versus COD curve of HA

increase and the load starts to decrease, the critical CMOD is about 40 µm with force 10 N. For CTOD curve can be divided to two parts, the first part the relationship is linear and the linearity continues until reach the peak load, after reach the peak load the crack opening increase with decrease the applied load. The critical CTOD is about 17 µm with force 10 N. The crack opening displacement continues to increase until the specimen fails.

The relationship between COD (CMOD and CTOD) and time shown in Fig. 12. From this figure can be notice the rate of crack opening was gradually until reach the critical time approximately 210 sec, the rate of crack opening increase comparison before critical time.
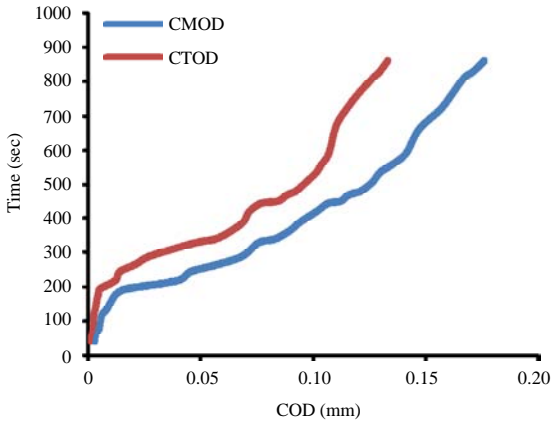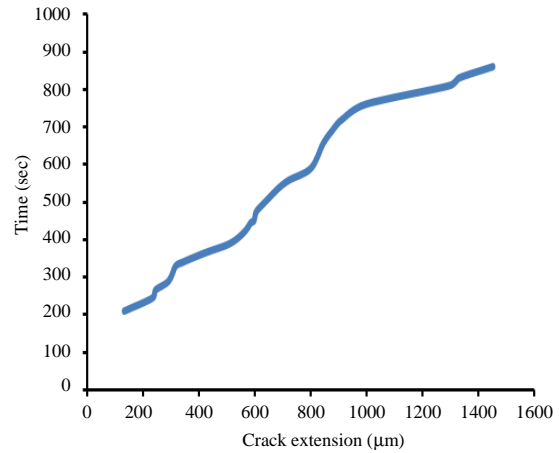
Fig. 12: Time versus COD curve of HA
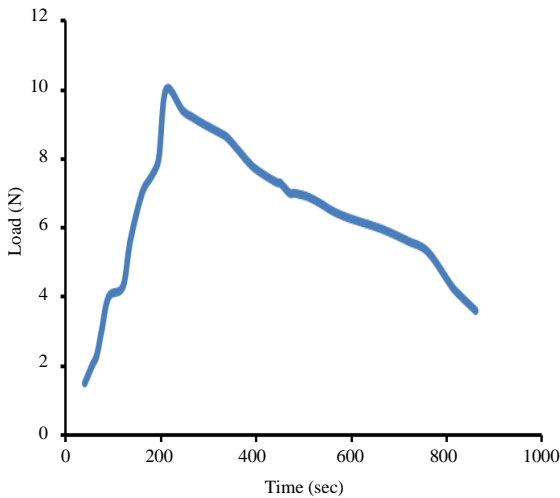

Fig. 13: Loads versus time curve of HA

Fig. 14: Force versus crack extension curve of HA

Crack propagation
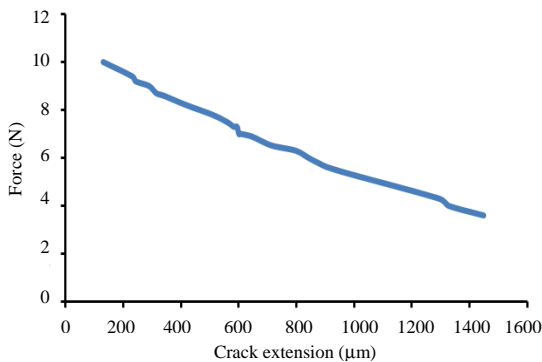
Crack propagation using strain mapping: Figure 13 shows the relationship between force and time in the

Fig. 15: Time versus crack extension curve of HA

Fig. 16: Crack opening profile above notch tip of HA for different loads

SENB method the peak load (10 N) called critical load F_{cr}. The time when crack initiation was 210 sec. The crack extension with load and time shown in Fig 14 and 15, respectively. Figure 14 shows the crack initiation at load 10 N and continues propagation with force >10 N; whereas Fig. 15 shows the crack start propagate at time 210 sec. The crack propagated in materials when energy available for crack extension is larger than the material's resistance to crack growth. For a perfectly brittle material such as hydroxyapatite, the energy available for crack growth is equal to the decrease in the system's elastic energy caused by the extension of the crack. This quantity is formally defined as the energy release rate G and this leads to break bonds between atoms

while the crack continues to growth when applied load produce energy larger than energy between atoms.

Crack observation using COD profile: Crack propagation can be also measured from crack opening profile as shown in Fig. 16. Form Fig. 16 can be notice that at load 8.6 N the crack opening along the crack approach to zero at height 346 μm where the result of crack propagation from strain change near the notch tip showing at load 8.6 N the crack extension is 340 μm. For load 7 N the crack extension from strain change near the notch tip was 601 μm whereas the crack extension from crack opening profile tend to be zero at height 607 μm. For load 4.3 N the crack extension from crack opening profile 1313 μm while with strain change was 1296 μm. This method can be considering as alternative method to measured crack propagation using strain map (previous method).

CONCLUSION

Study crack visualization, propagation and opening of HA play important role in determined durability and reliability in hydroxyapatite materials. The crack behavior of HA was calculation using SENB with assist DIC technique. The main conclusions can be summarized as follow:

- DIC technique proved a good method for revealed strain disruption and observation crack opening and propagation
- Critical load for nucleation crack in HA was 10 N
- Critical CMOD and CTOD of HA were 40 and 17 μm, respectively
- Critical time for nucleation crack was 210 sec
- Fracture toughness of HA using SENB method was 0.7 MPa $\sqrt{m}$

ACKNOWLEDGEMENTS

REFERENCES

Anstis, G.R., P. Chantikul, B.R. Lawn and D.B. Marshall, 1981. A critical evaluation of indentation techniques for measuring fracture toughness: I, direct crack measurements. J. Am. Ceramic Soc., 64: 533-538.

Berzina-Cimdina, L. and N. Borodajenko, 2012. Research of Calcium Phosphates using Fourier Transform Infrared Spectroscopy. In: Infrared Spectroscopy-Materials Science Engineering and Technology, Theophile, T. (Ed.). In Tech Publisher, Rijeka, Croatia, ISBN:978-953-51-0537-4, pp: 123-148.

Brynk, T., A. Laptiev, O. Tolochyn and Z. Pakiela, 2012. The method of fracture toughness measurement of brittle materials by means of high speed camera and DIC. Comput. Mater. Sci., 64: 221-224.

Brynk, T., A. Laptiev, O. Tolochyn and Z. Pakiela, 2014. Digital image correlation based method of crack growth rate and fracture toughness measurements on mini-samples. Key Eng. Mater., 586: 96-99.

Elghazel, A., R. Taktak and J. Bouaziz, 2015. Determination of elastic modulus, tensile strength and fracture toughness of bioceramics using the flattened Brazilian disc specimen: Analytical and numerical results. Ceram. Intl., 41: 12340-12348.

Eslami, H., M. Solati-Hashjin and M. Tahriri, 2008. Synthesis and characterization of nanocrystalline fluorinated hydroxyapatite powder by modified wet-chemical process. J. Ceram. Process. Res., 9: 224-229.

Kanninen, M.F., C.H. Popelar and A.J.M. Reviewer, 1986. Advanced fracture mechanics. J. Eng. Mater. Technol., 108: 1-1.

Li, W., T. Sakai, Q. Li and P. Wang, 2011. Statistical analysis of fatigue crack growth behavior for grade B cast steel. Mater. Des., 32: 1262-1272.

Lin, Z.X., Z.H. Xu, Y.H. An and X. Li, 2016. In situ observation of fracture behavior of canine cortical bone under bending. Mater. Sci. Eng. C, 62: 361-367.

Mathieu, F., F. Hild and S. Roux, 2012. Identification of a crack propagation law by digital image correlation. Intl. J. Fatigue, 36: 146-154.

Mekky, W. and P.S. Nicholson, 2006. The fracture toughness of Ni/Al2O3 laminates by digital image correlation I: Experimental crack opening displacement and R-curves. Eng. Fract. Mech., 73: 571-582.

Newman Jr, J.C., M.A. James and U. Zerbst, 2003. A review of the CTOA/CTOD fracture criterion. Eng. Fracture Mech., 70: 371-385.

Pattanayak, D.K., P. Divya, S. Upadhyay, R.C. Prasad and B.T. Rao *et al.*, 2005. Synthesis and evaluation of Hydroxyapatite ceramics. Trends Biomater Artif Organs, 18: 87-92.

Roux, S., J. Rethore and F. Hild, 2009. Digital image correlation and fracture: An advanced technique for estimating stress intensity factors of 2D and 3D cracks. J. Phys. D Appl. Phys., 42: 214004-214004.

Tagawa, T., Y. Kayamori, M. Ohata, T. Handa and T. Kawabata *et al.*, 2010. Comparison of CTOD standards: BS 7448-part 1 and revised ASTM E1290. Eng. Fract. Mech., 77: 327-336.

Tahriri, M., M. Solati-Hashjin and H. Eslami, 2008. Synthesis and characterization of hydroxyapatite nanocrystals via chemical precipitation technique. Iran. J. Pharm. Sci., 4: 127-134.

Triwatana, P., P. Srinuan and K. Suputtamongkol, 2013. Comparison of two fracture toughness testing methods using a glass-infiltrated and a zirconia dental ceramic. J. Adv. Prosthodontics, 5: 36-43.